Delayed emission of cold positronium from mesoporous materials

D. B. Cassidy, T. H. Hisakado, V. E. Meligne, H. W. K. Tom, and A. P. Mills Jr.
Department of Physics and Astronomy, University of California, Riverside, California 92521-0413, USA
(Received 17 September 2010; published 12 November 2010)

It is well known that ortho-positronium (ortho-Ps) atoms are emitted with high efficiency from various porous materials following the implantation of positrons. Since the ortho-Ps lifetime in a mesoporous material may be a substantial fraction of the ortho-Ps vacuum lifetime (142 ns), the time dependence of Ps emission may have to be considered when conducting certain types of experiments, such as time of flight measurements or pulsed ortho-Ps-laser interactions, when using this kind of target as a positronium source. By taking into account the positron implantation profile and subsequent Ps diffusion and decay in a mesoporous film we calculate the time dependent ortho-Ps emission rate $\Gamma(t)$, which in turn allows us to establish the total annihilation rate, arising from the decay of ortho-Ps both inside and outside the sample. Using time-delayed laser spectroscopy and single-shot lifetime measurements we have directly probed the rate at which Ps is emitted into vacuum from a target with ~3-nm diameter pores and have observed delayed ortho-Ps emission that is consistent with our model. From the ortho-Ps decay spectrum we find that, whereas a simple two-component lifetime fit gives a short lifetime of 25.3 ± 0.3 ns, an analysis that properly takes into account the emission rate yields an ortho-Ps lifetime inside the porous material of 32.3 ± 1.2 ns, demonstrating that the ortho-Ps escape rate into vacuum can significantly modify the apparent lifetime of ortho-Ps inside a mesoporous material. Our measurements yield a Ps diffusion coefficient $D = 0.07 \pm 0.01$ cm^2 s^{-1}, which is consistent with a tunneling limited diffusion process.

DOI: 10.1103/PhysRevA.82.052511 PACS number(s): 36.10.Dr, 34.80.Lx, 78.70.Bj

I. INTRODUCTION

The formation, diffusion, and lifetime of positronium (Ps) [1] in various porous materials [2] has been studied for many years [3,4], both as a way to characterize such materials (which, for example, may be useful as low-k dielectrics [5] in the semiconductor industry) and in the development of sources of Ps for fundamental physics experiments [6–8].

Positronium may be produced in porous materials following the implantation of a slow positron beam. Ps created in the bulk material diffuses until it either annihilates or reaches a pore. In the latter case Ps will be ejected into the void region (with ~1 eV or more [9]) and, after losing energy via collisions, will not be able to return to the bulk material and will thus be trapped in the pores [10]. The Ps lifetime in this environment depends on the interaction rate with the walls and therefore also on the pore size and the Ps mean free path [11–13]. Such Ps atoms will lose energy via collisions with the internal surfaces [14] and any impurities that may exist thereupon [15].

If the pores are interconnected Ps will diffuse between them and may reach the surface and be emitted into vacuum. The temperature of such emitted Ps will depend on the number of collisions with the walls that occur during this process and hence on the incident positron beam energy [16]. By capping the top layer of a porous film with a nonporous layer, Ps may be prevented from leaving the sample and be confined in the pore matrix. This approach allows one to study properties of porous films without complications arising from difficulties associated with differentiating between Ps annihilation inside and outside the target. However, it is not always convenient to apply a capping layer, and in some cases doing so may alter the very properties of the material one wishes to study [4].

The details of how Ps is able to diffuse through an interconnected porous network depend strongly on the nature of that structure. In particular, if the pore size is sufficiently small then the mechanisms by which Ps cooling and diffusion occur will change as the de Broglie wavelength becomes comparable to the pore diameter. Under these conditions the minimum Ps energy may be higher than would be expected simply by considering the ambient sample temperature due to the confinement energy in the pore [16–18]. Moreover, in this case diffusion becomes inhibited as Ps atoms are then only able to move from pore to pore by tunneling. This will typically be much slower than the random walk diffusion of a classical particle with average velocity $\bar{v}$ colliding with pores with average spacing λ, resulting in poor estimates of the Ps diffusion coefficient D based on the classical approximation $D \approx \bar{v}\lambda$ [19]. Indeed, although positronium is widely used as a probe of such materials, the details of how it moves from pore to pore in the quantum regime are frequently overlooked.

While the diffusion of positrons and positronium after implantation into a surface has been considered many times [20] and is well understood, there are significant details that should not be neglected when quantitative predictions are desired. One area where this may be important is in time-of-flight (TOF) experiments, wherein the time taken for Ps atoms to travel a fixed distance in vacuum is used to determine their energy. In this type of measurement the time at which the incident positron beam is implanted is usually taken to be the start time, and detection of an annihilation γ-ray photon (originating from a well-defined point a known distance from the target) defines the stop time. Thus, this methodology implicitly assumes that the time taken for Ps to be emitted into the vacuum is negligible compared to the flight time. If a sample with large pores or voids [21] is used it is likely that this will indeed be the case for relatively low implantation energies. However, if the positrons are implanted at an energy such that less than half the available Ps escapes

 ©2010 The American Physical Society

into vacuum before annihilating, then the mean emission time will be greater than half the mean Ps lifetime in the porous material [22]. The time taken for the majority of the Ps to be emitted into the vacuum will also depend critically on the initial Ps energy and subsequent cooling rate, since emission will be slowed when the Ps de Broglie wavelength is similar to the pore dimension. Thus, under some circumstances the time spent by Ps atoms in the sample prior to emission may have to be taken into account in order to properly interpret the data.

Another area where knowledge of the Ps emission time from a porous sample could be useful is in the production of large bursts of excited state Ps atoms, as may be required, for example, in the production of antihydrogen [23–27]. In such experiments, using cold Ps is generally advantageous as it helps reduce the Doppler broadened linewidth of the primary transition used to excite Ps from the ground state and hence will maximize its spectral overlap with the excitation laser.

In this article we present experimental verification of phenomena associated with delayed positronium emission. We first review in Sec. II the theory of Ps implantation, diffusion, and emission and present simple expressions for the total annihilation rate as a function of time, the mean time of emission, and other useful quantities. We describe our experimental arrangements in Sec. III and results in Sec. IV and conclude with a discussion in Sec. V.

II. CALCULATIONS

A. Ps formation and emission

The mean stopping depth of positrons implanted into a target of density ρ with kinetic energy K is given by [28]

$$\bar{z} = A\rho^{-1}K^{v}, \tag{1}$$

where K is in keV, $v \approx 1.7$, $A = 2.81\ \mu\text{g/cm}^2$ [29]. The implantation profile of positrons stopping at a mean depth $\bar{z}$ in a uniform solid may be written as [20]

$$P(z) = \frac{\pi z}{2\bar{z}^2}\exp\{-\pi z^2/4\bar{z}^2\}. \tag{2}$$

We suppose that a number of Ps atoms originate from a depth z at time $t = 0$ and then diffuse with a diffusion coefficient D while annihilating in the solid at a rate γ. The normalized distribution of Ps at depth x and time t after being formed (using a perfectly absorbing boundary condition at the surface) is [30]

$$\psi(z,x,t) = \theta(x)e^{-\gamma t}\int_0^\infty \frac{2}{\pi}\sin kz\sin kx\exp\{-Dk^2t\}\,dk, \tag{3}$$

where $\theta(x)$ is the unit step function. The rate of emission of Ps from the surface per initial Ps atom given the positron implantation profile $P(z)$ is

$$\begin{aligned}\Gamma(t,u) &= \int_0^\infty D\frac{\partial\psi(z,x,t)}{\partial x}\bigg|_{x=0+}P(z)\,dz \\ &= \frac{1}{2}\sqrt{u}e^{-\gamma t}[t+u]^{-3/2},\end{aligned} \tag{4}$$

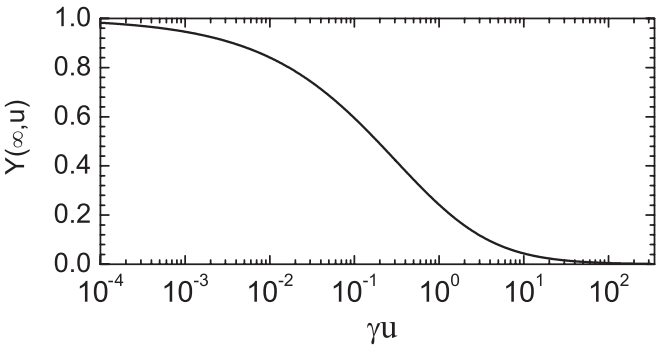

FIG. 1. The total yield of Ps in vacuum per initial Ps atom $Y(\infty,u)$ defined in Eq. (7) as a function of γu.

where

$$u = \bar{z}^2/\pi D. \tag{5}$$

The total Ps yield per initial Ps atom through time t is

$$\begin{aligned}Y(t,u) &= \int_0^t \Gamma(t',u)dt' \\ &= 1 - \sqrt{\pi\gamma u}e^{\gamma u}[erf\{\sqrt{\gamma(t+u)}\} - erf\{\sqrt{\gamma u}\}] \\ &\quad - e^{-\gamma t}[t/u+1]^{-1/2}.\end{aligned} \tag{6}$$

The total yield of Ps in vacuum per initial Ps atom is

$$Y(\infty,u) = 1 - \sqrt{\pi\gamma u}e^{\gamma u}erfc\{\sqrt{\gamma u}\}. \tag{7}$$

The behavior of $Y(\infty,u)$ as a function of γu is illustrated in Fig. 1.

Figure 2 shows the normalized rate $\Gamma(t)$ and Ps yield $Y(t)$ for different implantation energies, calculated using $\gamma = 30\ \mu\text{s}^{-1}$ and characteristic implantation energy at which $Y(\infty,u) = \frac{1}{2}$, $K_{1/2} = 5.8$ keV. The mean emission time is

$$\begin{aligned}\bar{t} &= \int_0^\infty t\Gamma(t,u)\,dt/Y(\infty,u) \\ &= \frac{\frac{1}{2}\gamma^{-1}\sqrt{\pi\gamma u}\exp\{\gamma u\}erfc\{\sqrt{\gamma u}\}}{1-\sqrt{\pi\gamma u}\exp\{\gamma u\}erfc\{\sqrt{\gamma u}\}} - u.\end{aligned} \tag{8}$$

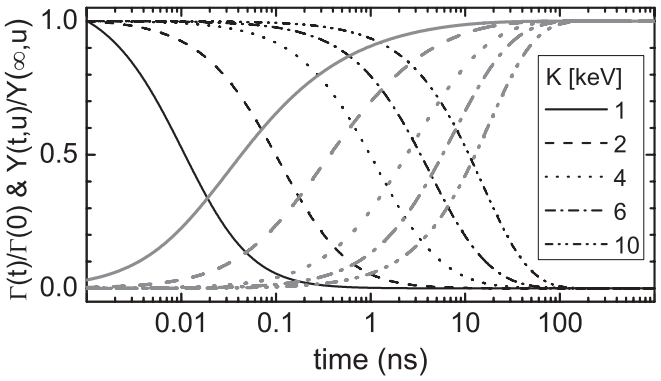

FIG. 2. Normalized emission rate $\Gamma(t)/\Gamma(0)$ (black lines) as defined in Eq. (4) and normalized yield $Y(t,u)/Y(\infty,u)$ (gray lines) defined in Eqs. (6) and (7) for different implantation energies K, calculated using $K_{1/2} = 5.8$ keV and $\gamma = 30\ \mu\text{s}^{-1}$.

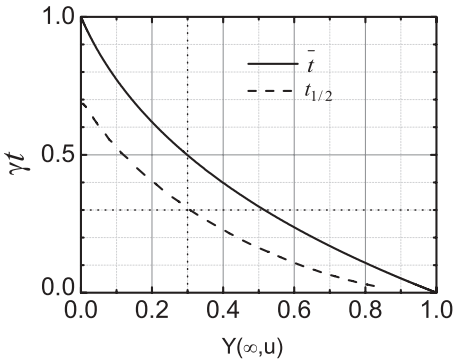

FIG. 3. Mean (solid curve) and median (dashed curve) times for Ps emission after positron implantation into a solid target surface for conditions such that the total yield per Ps atom $Y(t=\infty)$ is that given on the x axis. The dotted lines correspond to the example given in the text.

The median emission time $t_{1/2}$, which is the time at which half of the total amount of Ps that will escape has done so, satisfies

$$Y(t_{1/2},u)/Y(\infty,u) = \tfrac{1}{2}. \tag{9}$$

By solving this equation, $t_{1/2}$ may be inferred from the Ps yield if the Ps decay rate inside the sample is known. The mean and the median emission times are indicated in Fig. 3 to allow the reader to estimate the effects of delayed Ps. As an example, suppose the Ps mean lifetime in a sample is 50 ns and we wish to know at what time half the Ps escapes given an implantation energy at which the total Ps yield per Ps atom is 30% of the zero energy limit. At the intersection of the $t_{1/2}$ curve with a vertical line at normalized yield = 0.3 we find the time in units of 50 ns is 0.3. Thus the time for half the Ps to escape is ~15 ns, whereas the mean emission time is 25 ns. We emphasize, however, that significant Ps emission occurs over times with a range of an order of magnitude (see Fig. 2) so the time characteristic of the emission in one experiment may not be suitable for another. The long asymmetric tail of $\Gamma(t,u)$ also means that one's intuition about folding, means, and standard deviations, derived from work with symmetric Gaussian distributions, may be far from correct.

Solving Eq. (7) for $Y(\infty,u_{1/2}) = \frac{1}{2}$ leads to the condition $u_{1/2} \equiv 0.18727/\gamma$. Since the mean implantation depth is related to the implantation kinetic energy K by Eq. (1), and from the definition of u in Eq. (5), we have

$$D = \frac{A^2\rho^2}{0.18727\pi} K_{1/2}^{2\nu}\gamma, \tag{10}$$

which permits the diffusion coefficient to be derived from measurements of γ and $K_{1/2}$.

B. Ps decay rates with open pores

The difficulties associated with measuring the lifetime of Ps inside a porous material that also emits Ps into vacuum are well known [4]. One way in which this problem may be solved is to add a capping layer to prevent vacuum emission, so that only lifetimes resulting from Ps decay within the sample are measured. However, the capping layer can sometimes affect the measured lifetimes, either via Ps interactions with the boundary layer or by changing the structural properties of the sample. Moreover, it is not always possible (or desirable) to apply a capping layer to thin film samples.

In order to determine Ps lifetimes within a porous sample without capping Liszkay *et al.* [31] have devised a model in which the Ps decay inside and outside the sample is treated in a manner analogous to the well-known two-state trapping model (with a constant trapping rate) [32,33]. More complex models in which emission into the vacuum occurs describe this process with a time-dependent trapping rate [34,35]. The approach we take here is similar to this but is simplified by neglecting surface state trapping.

Let n_i and n_o be the fractions of the Ps atoms inside the sample and outside in vacuum, with time derivatives

$$dn_i/dt = -\Gamma(t) - \gamma n_i \tag{11}$$

and

$$dn_o/dt = \Gamma(t) - \gamma_o n_o, \tag{12}$$

where γ_o is the Ps decay rate outside the sample and $\Gamma(t)$ is the rate of Ps emission from the sample given by Eq. (4). Defining amplitudes as

$$n_{i(o)} = a_{i(o)}e^{-\gamma_{(o)}t} \tag{13}$$

we see that

$$da_i/dt = -\Gamma(t)e^{\gamma t}, \tag{14}$$

which has the solution

$$a_i(t) = 1 - \int_0^t \Gamma(x)e^{\gamma x}dx, \tag{15}$$

since the fraction of the particles that are inside at $t=0$ is 1. The other amplitude satisfies

$$da_o/dt = \Gamma(t)e^{\gamma_o t}, \tag{16}$$

which has the solution

$$a_o(t) = \int_0^t \Gamma(x)e^{\gamma_o x}dx. \tag{17}$$

The total annihilation rate from decays both inside and outside the sample is thus

$$\begin{aligned} S(t) &= \gamma n_i(t) + \gamma_o n_o(t) \\ &= \gamma e^{-\gamma t}\left[1 - \int_0^t \Gamma(x)e^{\gamma x}dx\right] + \gamma_o e^{-\gamma_o t}\int_0^t \Gamma(x)e^{\gamma_o x}dx \\ &= \gamma e^{-\gamma t}\sqrt{\frac{u}{t+u}} + \gamma_o e^{-\gamma_o t}Y(t,u,\gamma-\gamma_o). \end{aligned} \tag{18}$$

The total annihilation rate $S(t)$ is shown in Fig. 4 calculated for various different positron beam implantation energies, K. At low K the positrons spend so little time in the sample that the decay curve is almost a single exponential, except the rate is faster at short times due to the rapid escape of the Ps atoms that were implanted close to the surface. The most pronounced effect occurs for $K > K_{1/2}$ where it takes more than 100 ns to reach a steady-state decay rate.

It should be pointed out that we have not taken into account the effects of nonthermal Ps in the above considerations.

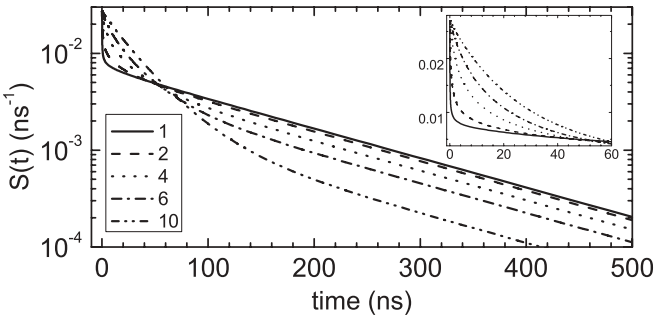

FIG. 4. Total annihilation rate (inside and outside the sample) for different positron beam energies (shown in the legend in keV) as determined from Eq. (18), calculated for $K_{1/2} = 5.8$ keV. The inset shows an expansion of the first 60 ns.

In the case of our particular sample we know that Ps does not thermalize [36] for beam implantation energies below ~2 kV [16] and so our analysis will not be correct for these low energies. Furthermore, for any beam implantation energy there will always be some component of Ps emission due to nonthermal atoms that will modify the overall emission rate. The extent to which this occurs may be estimated by considering the relative overlap of the implantation profiles for thermal and nonthermal Ps. We estimate that corrections arising from this will be of the order of 10% or less, decreasing with higher beam implantation energies. It would not be possible to obtain analytical solutions, as we have done here, if Ps cooling were included in the model. In that case one would have to resort to numerical solutions that are beyond the scope of the present work.

III. EXPERIMENT

In the present experiments a positron trap [37] and accumulator [38] were used to produce positron pulses containing around 2×10^7 particles with a spot size of ~1 mm. The pulses were bunched [39] to ~1 ns [full width at half maximum (FWHM)] using a high voltage buncher and could be implanted into the target material with energies ranging from 1 to 7 keV [40]. The positrons were implanted into a silica film whose ~3-nm diameter pores were interconnected up to the film surface. These kinds of targets produce Ps with high efficiency (~50%) that is able to escape into vacuum [16,18]. The amount of such Ps that is emitted into the vacuum depends on the positron implantation energy (among other things).

The decay of Ps formed in this way was observed via its annihilation radiation using a single-shot lifetime method [41] with either a PbF_2 Cherenkov radiator or a $PbWO_4$ scintillator [42] attached to a photomultiplier tube (PMT). The Cherenkov radiator has excellent timing properties but is quite inefficient and so this detector was used only to obtain lifetime spectra when the actual lifetime information was required. In this case multiple shots had to be averaged. The $PbWO_4$ has a relatively long decay time (~15 ns) and was used primarily to measure changes in the total amount of long-lived Ps present following laser-Ps interactions. Details of Ps formation and cooling in the sample as well as the basic experimental methods used are explained in detail in Ref. [16].

Single-shot lifetime spectra were used to obtain the delayed fraction, f_d, of our lifetime spectra. We define this as

$$f_d = \int_{50\ \mathrm{ns}}^{300\ \mathrm{ns}} V(t)\,dt \Big/ \int_{-50\ \mathrm{ns}}^{300\ \mathrm{ns}} V(t)\,dt, \tag{19}$$

where $V(t)$ is the PMT output voltage. This parameter is related to the triplet Ps fraction, f_3 (i.e., the fraction of incident positrons annihilating as triplet Ps) via $f_3 \approx A f_d$, where $A \approx e^{t/\tau} = 1.42$, since $t = 50$ ns (the lifetime spectrum cutoff) and $\tau \sim 142$ ns (the Ps mean lifetime in vacuum).

Laser spectroscopy of Ps was performed via the $1S$-$2P$ transition with a ~4 ns duration fixed wavelength 242.95-nm (in air) pulse [16,43] and subsequent photoionization [44] with a ~7 ns duration 532-nm pulse. Photoionization leads to a reduction in f_d because it liberates an electron from a Ps atom and increases the annihilation rate compared to the long-lived triplet Ps state. The Ps density vs. time was measured via the change in f_d as a function of time delay between the positron implantation pulse and the photoionization pulses.

A schematic of the optical layout of the laser system is shown in Fig. 5. A Surelite III-10 Q-switched Nd:YAG laser with phase-matched KD*P second- and third-harmonic generators was used to provide 532- and 355-nm pulses. This laser was pumped by flash lamps triggered at 10 Hz in order to keep the temperature of the laser and YAG rod stable, but the Q switch was fired only in coincidence with the positron beam as required at ~0.007 Hz. The ~7 ns duration, 40-mJ, 532-nm pulse was time delayed to arrive at the target at the same time as the 243-nm pulse. The ~7-ns duration, 120-mJ, 355-nm pulse was used to pump a Spectra-Physics PDL-1 dye laser with the grating set at first order Littrow using LD 489 dye (Exciton) to produce broadband 486-nm pulses. The 486-nm output was frequency doubled in a Type I phase-matched β-barium borate (BBO) crystal to produce ~4-ns duration, 400-μJ pulses at 243 nm. The 243-nm wavelength and bandwidth were characterized

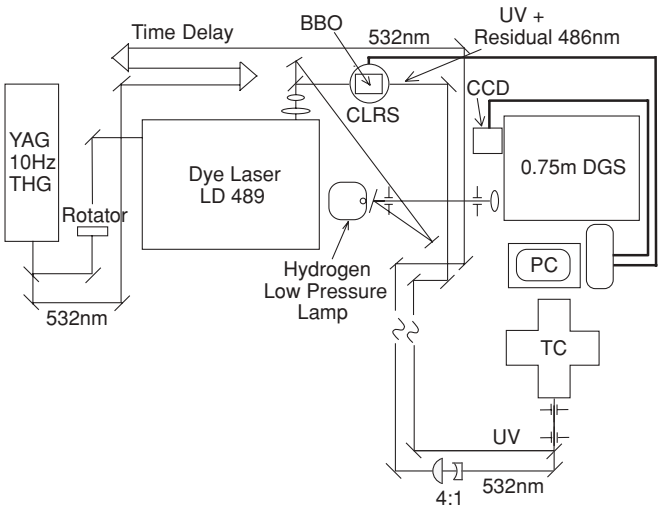

FIG. 5. Optical layout of the laser systems. CLRS refers to the closed loop rotational stage, DGS to the diffraction grating spectrometer, and TC to the target chamber in which the Ps is formed.

before and after a run using ~0.1% of the 486-nm light in a SPEX 0.75-m diffraction grating spectrometer operated at $f/8$ with a 1200-line/mm grating in second order with a CCD array camera at the exit slit. The dye laser output and light from a low-pressure hydrogen lamp were overlapped using a partially transmitting mirror (see Fig. 5) and made collinear to better than 50 μ rad and focused on the entrance slit of the spectrometer. The 486-nm pulse from the dye laser and the Balmer H-β line ($\lambda = 486.139$ nm) were detected simultaneously on the CCD array. This arrangement gave an absolute wavelength uncertainty of ~0.02 nm, limited by drift and the collinear alignment of the H-line. Wavelength differences on the CCD array were calibrated using multiple lines from a Mercury and Argon light source which could also be made collinear to the other inputs. The resolution in this arrangement was 0.005 nm due to the finite pixel size on the CCD camera and the spectrometer resolution. The 486-nm pulse linewidth was fit to a Gaussian profile and measured to be 94 ± 10 GHz (FWHM). The acceptance bandwidth of the BBO was 500 GHz (FWHM) and the phase-matching angle of the BBO crystal was computer controlled to track the dye laser so the SHG output frequency can be considered to be ideally doubled over the 94-GHz bandwidth. The 243-nm pulse was then calculated to have a 133 ± 14 GHz (FWHM) linewidth with a center frequency uncertainty of ± 0.01 nm (50 GHz).

IV. MEASUREMENTS

Our model for Ps emission concerns three processes, namely Ps decay (both inside and out of the sample) and the Ps emission rate, which depends on the Ps diffusion coefficient D and mean positron implantation depth $\bar{z}$. By measuring the total decay rate with a fast detector and the Ps emission rate via laser spectroscopy, we obtain two independent data sets. Together these are sufficient to find the two decay rates as well as the parameter $u = \bar{z}^2/\pi D$.

A. Decay rates

The total decay rate of Ps was measured using the technique of single-shot positron annihilation lifetime spectroscopy (SSPALS) [41]. In order to obtain good time resolution a small 20×20 mm cylindrical PbF_2 Cherenkov detector attached to a microchannel plate (MCP) PMT was used [42]. This detector has a time resolution of less than 2 ns, but the small size of the Cherenkov radiator, as well as the intrinsic inefficiency of this method of measuring low-energy γ rays, means that many shots had to be averaged to obtain good statistics. In the present case 70 shots were averaged, which took approximately 2 h.

Figure 6 shows two such spectra, recorded using a beam impact energy of 6.2 keV, with a silica film as well as a phosphor screen as targets. The latter is usually used for imaging the beam but in this case serves as a good representation of the system response function as very little Ps formation is expected. In these spectra there is a pulse that occurs ~10 ns after the prompt peak at $t = 0$ which is apparently caused by feedback of light from the PMT anode to its photocathode. We remove this effect from the spectra

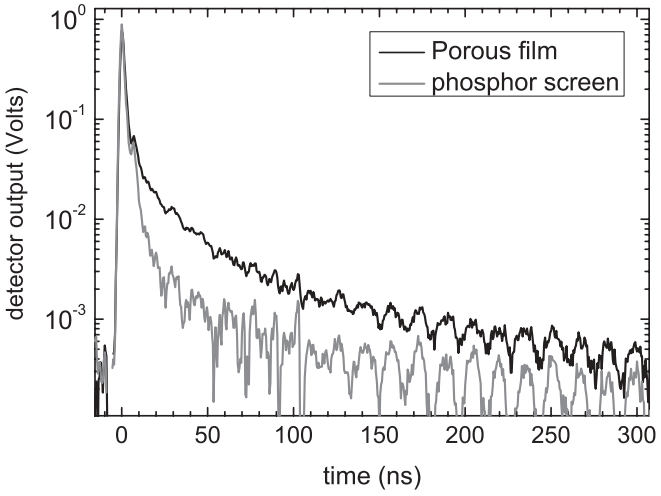

FIG. 6. Average of 70 single-shot lifetime spectra recorded using a PbF_2 Cherenkov radiator attached to a fast PMT. The phosphor screen data is used as a resolution function since very little Ps formation is expected using this target. The mean positron implantation energy is 6.2 keV.

by subtracting from the raw data a delayed copy of the data with amplitude and delay time chosen to optimally remove the feedback pulse. Low-amplitude oscillations evident at larger delay times are caused by impedance mismatches at the ends of the cable connecting the detector to the oscilloscope and by the variations of the cable properties along its length [42].

Let us represent the ideal lifetime distribution $S'(t)$ corresponding to the porous film data of Fig. 6 as the sum of a prompt peak $\delta(t)$ plus a delayed curve $d(t)$:

$$S'(t) = \delta(t) + d(t). \tag{20}$$

The resolution $R(t)$ represented by the phosphor screen curve of Fig. 6 is modelled as the sum of a narrow unit area prompt portion $p(t)$ plus a small amplitude delayed portion $r(t)$:

$$R(t) = p(t) + r(t). \tag{21}$$

The measured lifetime curve becomes

$$L(t) = R(t) \otimes S(t) = p(t) + d(t) + r(t) + d(t) \otimes r(t), \tag{22}$$

where $\otimes$ represents the operation of folding two distributions, and we assume $p(t) \otimes d(t) \approx d(t)$. Neglecting the last term on the right because of its small amplitude, we see that we may obtain a close approximation to the true lifetime curve for the porous film by simply subtracting the two peak area normalized spectra in Fig. 6, the supposition being that the reflections were proportional to the peak areas and of the same shape for both spectra since the apparatus was undisturbed between the two measurements. The difference curve is shown in Fig. 7, sans the peak region for $t < 10$ ns.

A fit to the data of Fig. 7 using the $S(t)$ curve of Eq. (18) requires optimization of five parameters: γ, γ_o, $u = \bar{z}^2/\pi D$, an overall multiplicative constant, and a constant b multiplying the second term of $S(t)$ to account for the ~30% relative efficiency of the PbF_2 detector for three photon annihilations vs. two photon annihilations [42]. Since the χ^2 for the fit is

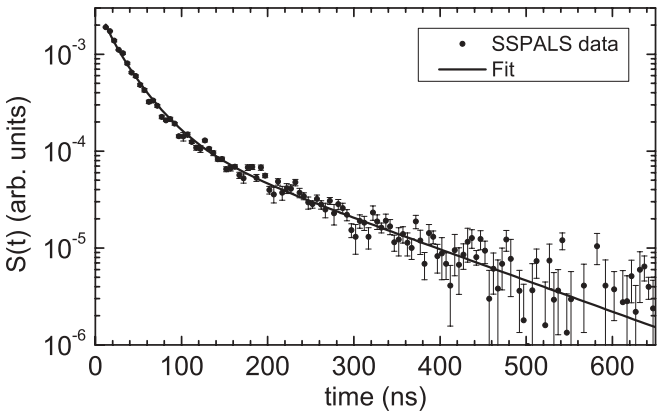

FIG. 7. Lifetime spectra obtained from data of Fig. 6. The solid line is a fit to the function defined by Eq. (18).

insensitive to the value of u, we obtain the fitted value of γ for various trial values of u, with the results indicated by the filled circle data in Fig. 8. The ambiguity in u will be resolved by the laser measurement of the emission rate presented in the next subsection. The constant b determined by the final fit turns out to be $30 \pm 2\%$.

B. Emission rate

We have measured the Ps fraction f_d as a function of the time at which a resonant probe laser is fired with respect to the implantation of an intense positron pulse. That is, we have measured the amount by which the Ps fraction changes due to laser excitation and ionization as a function of time after the Ps has been created, $\Delta f_d(t)$. From this we obtain information regarding the amount of Ps in vacuum as a function of time: Since the probe laser was close to the target surface, the Ps is probed just as it is leaving the film, and $\Delta f_d(t)$ is in effect a measurement of the emission rate. There are, however, a

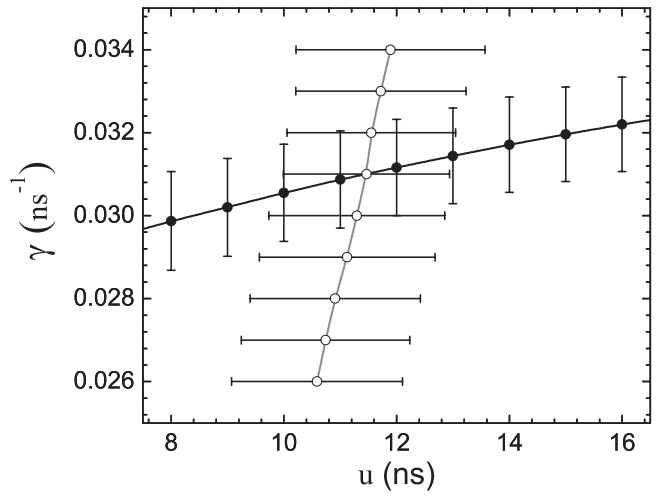

FIG. 8. Mutual dependence of the decay rate γ of Ps in the porous silica sample as a function of the parameter u. The lifetime data (filled circles) were taken at $K = 6.2$ keV, while the delayed emission data (open circles) were obtained with $K = 4.96$ keV. The values of u for the latter have been multiplied by 2.135 to correspond to what would be expected at $K = 6.2$ keV.

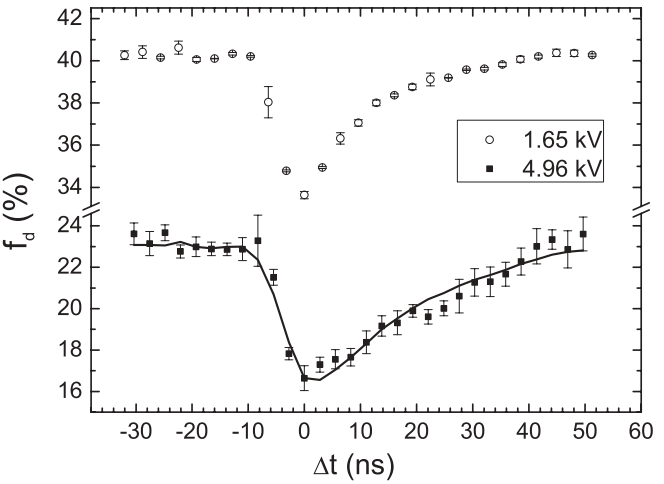

FIG. 9. Laser excitation measurement as a function of laser delay time. The laser beam was parallel to the sample surface and its midpoint was ~1 mm from the surface. The solid line over the 4.96-keV data is the calculated Ps emission rate of Eq. (4) folded with the 1.65-keV measurement, which is taken to be the system response.

few complicating factors in this measurement. First, Ps that is emitted at early times will be hotter and will therefore have less overlap with the excitation laser due to Doppler broadening. For these hot atoms then, the yield does not have quite the same proportionality to the amount of Ps present as for thermal [36] Ps. Second, because the laser was ~1 mm in front of the sample there will be some time-of-flight component to our measurement, which broadens the effective resolution. Finally, the time width of the laser pulses (~7 ns convoluted) also reduces the resolution of the measurement. Nevertheless, we were able to obtain a clear indication of delayed Ps emission.

Measurements at two mean positron implantation energies, 1.65 and 4.96 keV, are shown in Fig. 9 using laser pulses that were ~7 ns wide. The 243-nm $1S$-$2P$ excitation laser beam and the $2P$-state-photoionizing 532-nm laser beam were directed parallel to the sample surface and centered about 1 mm from the surface. Thus, the Ps is being excited (and then detected) almost immediately after emerging from the surface. One may therefore expect that the time-dependent delayed fraction signal in Fig. 9 should be proportional to the Ps emission rate $\Gamma(t,u)$ given in Eq. (4).

The low implantation energy measurement corresponds to Ps reaching the surface in less than 1 ns and therefore may be taken to represent the overall system time response. The measurements at 4.96 keV are clearly showing the effect of delayed emission of the Ps. The data are fitted by a curve proportional to $\Gamma(t,u)$ folded with the 1.65-keV measurement. The best fit values of u found for various values of γ show that the fitted value of u is almost independent of the value chosen for γ. While the separate fits to the data of Figs. 7 and 9 are not themselves sufficient to determine both γ and u, the combined results are. Before doing this we must correct for the fact that the lifetime data were obtained with $K = 6.2$ keV, while the delayed emission data were obtained at $K = 4.96$ keV. We correct the u values for the latter by multiplying them by

$(6.2/4.96)^{3.4} = 2.135$, resulting in the open circle data in Fig. 8. The intersection of the two data sets in Fig. 8 then gives us $\gamma = 31.0 \pm 1.2\ \mu s^{-1}$ and $u = 11.5 \pm 1.5$ ns at $K = 6.2$ keV. The curve through the 4.96-keV measurements indicates the best fit to the delayed emission data in Fig 9. We note that due to the ~10-ns time resolution, data recorded at the edge of the f_d integration region cutoff at 50 ns will underestimate the signal. This is most likely the reason why the fit and the data may be starting to diverge slightly. We conclude that the mean lifetime inside the sample is $1/\gamma = 32.3 \pm 1.2$ ns. On the other hand, a simple two-lifetime fit yields $\tau_1 = 25.3 \pm 0.3$ ns and $\tau_2 = 140 \pm 7$ ns with a fitted curve essentially indistinguishable from the one in Fig 7. One sees that the apparent 25-ns short lifetime arises from the inside decay rate augmented by the rate for Ps to escape into the vacuum, just as in the usual two state trapping model [32,33], with the added complication of there being a range of diffusion times for the Ps to reach the surface where it escapes into the effective trap (i.e., the vacuum).

Using a density of the porous silica of 1.35 g/cm^3, we find from Eq. (1) that the mean positron implantation depth at $K = 6.2$ keV is $\bar{z} = 463$ nm. The diffusion coefficient of Ps within the target is then $D = \bar{z}^2/\pi u = 0.065 \pm 0.012$ cm^2 s^{-1}. On the other hand, we may use Eq. (10) to find the diffusion coefficient from the implantation energy $K_{1/2}$ at which the total Ps yield falls to half its value at zero energy.

We measure $K_{1/2} = 5.8$ keV and thus $D = 0.08 \pm 0.01$ cm^2 s^{-1} in agreement with the determination based on the fitted value of u above. Averaging the two values gives $D = 0.07 \pm 0.01$ cm^2 s^{-1}, with a conservative error estimate to allow for possible systematic effects. The fact that we are able to understand the two entirely different measurements of Figs. 7 and 9 using the same values of lifetime and diffusion coefficient may be taken as an indication that our simple theory may be used as an adequate predictor for these delayed Ps emission experiments.

A commonly used (e.g., Ref. [16]) method to estimate the diffusion coefficient is simply to assume that for a beam implantation energy $K = K_{1/2}$ the mean implantation depth is given by

$$\bar{z}_{1/2} = \sqrt{2D\tau_r} \equiv \sqrt{2D\kappa\tau} \tag{23}$$

from elementary diffusion theory [45–47]. Here τ_r is a residence time which is usually assumed to be some fraction κ of the Ps lifetime in the material. Although on occasion values of $\kappa = 0.25$, 0.5, or 1 have been used to obtain estimates of D, agreement with Eq. (10) requires $\kappa = 0.29416$.

V. DISCUSSION

Our description of delayed Ps emission from porous films does not explicitly address the mechanisms by which the Ps emission times are extended. Rather, the Ps emission is described in terms of a diffusion coefficient and mean implantation depth, the values of which will set the time scale for Ps emission. The diffusion coefficient itself may be much smaller than expected classically because, as Ps cools down in small pores its de Broglie wavelength will eventually become comparable to the pore size, and diffusion will then proceed through tunneling, which will be much slower than a classical point particle bouncing off the pore walls.

As an example, for Ps atoms at thermal energies in a porous film the diffusion coefficient D is sometimes approximated to be $d \times \bar{v}$, where d is the pore diameter and the mean thermal velocity $\bar{v} \sim 1 \times 10^7$ cm/s [e.g., Refs. [22,48]]. For 3-nm pores this gives $D \sim 3$ cm^2/s. However, in our sample with $d \sim 3$ nm we obtained a diffusion coefficient of 0.07 ± 0.01 cm^2/s, more than an order of magnitude lower. Thus, it is obvious that one cannot always ignore the quantum nature of cold Ps in a cavity.

To see how Ps might move in a porous material at low energies, we have calculated the time required for a Ps atom to tunnel from one pore to the next in a model system consisting of two spherical pores connected by a narrow channel [16]. We calculated the binding energies for the lowest symmetric and antisymmetric states assuming an axially symmetric cavity with an infinite repulsive potential at the walls. For the case of a 1.2-nm diameter connection between a pair of 2.4-nm diameter spherical pores, separated by a center-to-center distance $\Lambda = 3.2$ nm, the symmetric ground-state binding energy is 108 meV and the symmetric-antisymmetric energy splitting is $\delta E = 0.833$ meV. The time to tunnel from one pore to the next is $\Delta t = h/2\delta E = 5$ ps, to be compared with the time for a thermal velocity Ps atom to travel a distance Λ, $\Delta t_{\rm th} = \Lambda/v_{\rm th} = 50$ fs. This gives a thermal diffusion coefficient for tunneling transport [19] $D = \Lambda^2/2\Delta t_{\rm th} \approx 0.01$ cm^2 s^{-1}. Opening the connecting link to a diameter of 1.7 nm lowers the ground-state binding energy to 104 meV and increases the energy splitting to 3.66 meV and the diffusion coefficient to ~0.04 cm^2 s^{-1}. The exact values of these parameters will depend on the properties of any given sample, but this estimate indicates that our measured D is consistent with a tunneling limited diffusion process.

The slow emission of Ps from mesoporous materials does not mean that TOF methods cannot be used, only that for a given experimental arrangement it should be determined if the emission time is indeed negligible, or if it should be taken into account [49]. In the latter case, simply adjusting the flight time by the median emission time could be inadequate, and one might have to model the complete emission profile in order to obtain accurate results (in addition to any other modeling, such as Ps cooling, detection efficiencies, etc., Refs. [16,18]).

Pulsed laser spectroscopy of Ps relies on maximizing the laser overlap with the available Ps in the temporal, spatial, and spectral domains. If Ps is formed from a metal surface [50,51] then it will be emitted at approximately thermal temperatures in a time that will likely depend mostly on the width of the initial positron pulse (since the positron surface state lifetime on a metal is typically of the order of 0.5 ns [52]). Since metals can be difficult to keep clean, porous films (or similar materials [53]) as an alternative source of Ps have many advantages, not the least of which is that they are essentially maintenance free. They can emit Ps with high efficiency at low temperatures [18,49] which makes them attractive for possible use in some proposed antihydrogen experiments [23–27], which are necessarily conducted in cryogenic (4.2 K) antiproton traps [54,55]. For such experiments, where Rydberg

Ps is required, one would implant a positron beam at an energy designed to simultaneously optimize the emission and excitation of Ps. Similarly, it would also be advantageous to tailor the time width of the excitation laser according to the resulting Ps emission profile, even if the incident positron pulse is short.

To conclude, we have experimentally demonstrated the delay in emission of Ps from a porous film and shown that our measurements are in agreement with a simple diffusion theory. The results are expected to be relevant and important for TOF measurements, the production of bursts of excited state Ps, and interpreting positronium lifetime spectra associated with porous materials.

ACKNOWLEDGMENTS

We are grateful to R. G. Greaves for discussions, to P. Crivelli, L. Liszkay, P. Perez, and coworkers for providing porous silica samples, and to an anonymous referee for very helpful comments. This work was supported in part by the National Science Foundation under Grant No. PHY 0900919 and by the US Air Force Research Laboratory.

[1] Note that throughout this article we shall discuss only ortho-Ps and, for brevity, we shall refer to this simply as Ps.
[2] Y. Kobayashi, K. Ito, T. Oka, and K. Hirata, Radiat. Phys. Chem. **76**, 224 (2007).
[3] R. Paulin and G. Ambrosino, J. de Physique **29**, 263 (1968).
[4] D. W. Gidley, H. G. Peng, and R. S. Vallery, Annu. Rev. Mater. Res. **36**, 49 (2006).
[5] D. W. Gidley, K. G. Lynn, M. P. Petkov, J. N. Sun, M. H. Weber, and A. F. Yee, in *New Directions in Antimatter Chemistry and Physics*, edited by C. M. Surko and F. A. Gianturco (Kluwer, Dordrecht, 2001), p. 151.
[6] D. B. Cassidy, S. H. M. Deng, R. G. Greaves, T. Maruo, N. Nishiyama, J. B. Snyder, H. K. M. Tanaka, and A. P. Mills Jr., Phys. Rev. Lett. **95**, 195006 (2005).
[7] D. B. Cassidy and A. P. Mills Jr., Phys. Rev. Lett. **100**, 013401 (2008).
[8] D. B. Cassidy, V. E. Meligne, and A. P. Mills Jr., Phys. Rev. Lett. **104**, 173401 (2010).
[9] Y. Nagashima, Y. Morinaka, T. Kurihara, Y. Nagai, T. Hyodo, T. Shidara, and K. Nakahara, Phys. Rev. B **58**, 12676 (1998).
[10] E.g., M. P. Petkov, C. L. Wang, M. H. Weber, K. G. Lynn, and K. P. Rodbell, J. Phys. Chem. **107**, 2725 (2003).
[11] S. J. Tao, J. Chem. Phys. **56**, 5499 (1972).
[12] M. Eldrup, D. Lighbody, and J. N. Sherwood, Chem. Phys. **63**, 51 (1981).
[13] D. W. Gidley, W. E. Frieze, T. L. Dull, A. F. Yee, E. T. Ryan, and H.-M. Ho, Phys. Rev. B **60**, R5157 (1999).
[14] E.g., H. Saito and T. Hyodo, in *New Directions in Antimatter Chemistry and Physics*, edited by C. M. Surko and F. A. Gianturco (Kluwer, Dordrecht, 2001), p. 101.
[15] C. He, T. Ohdaira, N. Oshima, M. Muramatsu, A. Kinomura, R. Suzuki, T. Oka, and Y. Kobayashi, Phys. Rev. B **75**, 195404 (2007).
[16] D. B. Cassidy, P. Crivelli, T. H. Hisakado, L. Liszkay, V. E. Meligne, P. Perez, H. W. K. Tom, and A. P. Mills Jr., Phys. Rev. A **81**, 012715 (2010).
[17] S. Mariazzi, A. Salemi, and R. S. Brusa, Phys. Rev. B **78**, 085428 (2008).
[18] P. Crivelli, U. Gendotti, A. Rubbia, L. Liszkay, P. Perez, and C. Corbel, Phys. Rev. A **81**, 052703 (2010).
[19] Note that for a particle diffusing in one dimension with an exponentially distributed path length between scattering events, the diffusion coefficient is given by $D = \bar{v}\lambda$, where λ is the mean free path. For hopping in one dimension from pore to pore with a fixed path length Λ, $D = \frac{1}{2}\bar{v}\Lambda$,. See, e.g., F. Reif, *Fundamentals of Statistical and Thermal Physics* (McGraw-Hill, New York, 1965), p. 485.
[20] P. J. Schultz and K. G. Lynn, Rev. Mod. Phys. **60**, 701 (1988).
[21] A. P. Mills Jr., E. D. Shaw, R. J. Chichester, and D. M. Zuckerman, Phys. Rev. B **40**, 2045 (1989).
[22] H. K. M. Tanaka, T. Kurihara, and A. P. Mills Jr., Phys. Rev. B **72**, 193408 (2005).
[23] P. Perez and A. Rosowsky, Nucl. Instrum. Methods A **532**, 523 (2004).
[24] A. Kellerbauer *et al.*, Nucl. Instrum. Methods B **266**, 351 (2008).
[25] M. Doser *et al.* (AEGIS Collaboration), J. Phys. Conf. Ser. **199**, 012009 (2010).
[26] R. Ferragut, A. Calloni, A. Dupasquier, G. Consolati, F. Quasso, M. G. Giammarchi, D. Trezzi, W. Egger, L. Ravelli, and M. P. Petkov, J. Phys. Conf. Ser. **225**, 012007 (2010).
[27] F. Castelli, I. Boscolo, S. Cialdi, M. G. Giammarchi, and D. Comparat, Phys. Rev. A **78**, 052512 (2008).
[28] A. P. Mills Jr. and R. J. Wilson, Phys. Rev. A **26**, 490 (1982).
[29] J. Algers, P. Sperr, W. Egger, G. Kögel, and F. H. J. Maurer, Phys. Rev. B **67**, 125404 (2003).
[30] A. P. Mills Jr. and C. A. Murray, Appl. Phys. **21**, 325 (1980).
[31] L. Liszkay, C. Corbel, L. Raboin, J.-P. Boilot, P. Perez, A. Brunet-Bruneau, P. Crivelli, U. Gendotti, A. Rubbia, and T. Ohdaira, Appl. Phys. Lett. **95**, 124103 (2009).
[32] W. Brandt, in *Positron Annihilation*, edited by A. T. Stewart and L. O. Roellig (Academic Press, New York, 1967), p. 155.
[33] P. Hautojärvi and C. Corbel in *Proceedings of the International School of Physics*, Course CXXV, Positron Spectroscopy of Solids, edited by A. Dupasquier and A. P. Mills (IOS, Amsterdam, 1995), pp. 491–532.
[34] W. E. Frieze, K. G. Lynn, and D. O. Welch, Phys. Rev. B **31**, 15 (1985).
[35] D. T. Britton, J. Phys.: Cond. Mat. **3**, 681 (1991).
[36] It is not strictly accurate to refer to thermal Ps in the sample we discuss here; the small pore size means that Ps cannot cool to an energy that is lower than the Ps confinement energy in the pores (see Refs. [16-18]). However, once Ps has reached this minimum energy it will have a constant diffusion coefficient and so may be considered to be "thermal" for the present purposes.
[37] C. M. Surko and R. G. Greaves, Phys. Plasmas **11**, 2333 (2004).
[38] D. B. Cassidy, S. H. M. Deng, R. G. Greaves, and A. P. Mills Jr., Rev. Sci. Instrum. **77**, 073106 (2006).
[39] A. P. Mills Jr., Appl Phys. **22**, 273 (1980).

[40] One of the disadvantages of using a high-voltage buncher is that there is a minimum beam energy one can use. In this case it was ∼1 keV.
[41] D. B. Cassidy, S. H. M. Deng, H. K. M. Tanaka, and A. P. Mills Jr., Appl. Phys. Lett. **88**, 194105 (2006).
[42] D. B. Cassidy and A. P. Mills Jr., Nucl. Instrum. Methods A **580**, 1338 (2007).
[43] K. P. Ziock, C. D. Dermer, R. H. Howell, F. Magnota, and K. M. Jones, J. Phys. B **23**, 329 (1990).
[44] M. S. Fee, A. P. Mills Jr., E. D. Shaw, R. J. Chichester, D. M. Zuckerman, S. Chu, and K. Danzmann, Phys. Rev. A **44**, R5 (1991).
[45] See, for example, R. K. Pathria, *Statistical Mechanics*, 2nd ed. (Butterworth-Heinemann, Oxford, 1996), p. 461.
[46] A. Einstein, Ann. Phys. **17**, 549 (1905).
[47] M. Smoluchowski, Ann. Phys. **21**, 756 (1906).
[48] H. K. M. Tanaka, T. Kurihara, and A. P. Mills, J. Phys. Condens. Matter **18**, 8581 (2006).
[49] S. Mariazzi, P. Bettotti, and R. S. Brusa, Phys. Rev. Lett. **104**, 243401 (2010).
[50] K. F. Canter, A. P. Mills Jr., and S. Berko, Phys. Rev. Lett. **33**, 7 (1974).
[51] A. P. Mills Jr. and L. Pfeiffer, Phys. Rev. Lett. **43**, 1961 (1979).
[52] K. G. Lynn, W. E. Frieze, and P. J. Schultz, Phys. Rev. Lett. **52**, 1137 (1984).
[53] S. Mariazzi, P. Bettotti, S. Larcheri, L. Toniutti, and R. S. Brusa, Phys. Rev. B **81**, 235418 (2010).
[54] G. Gabrielse *et al.* (ATRAP Collaboration), Phys. Rev. Lett. **100**, 113001 (2008).
[55] G. B. Andresen *et al.* (ALPHA Collaboration), Phys. Rev. Lett. **105**, 013003 (2010).